DOI: 10.1002/anie.201003875

Mesoporous Crystals

Self-Consistent Structural Solution of Mesoporous Crystals by Combined Electron Crystallography and Curvature Assessment**

Keiichi Miyasaka and Osamu Terasaki*

Mesoporous crystals (MCs) are fascinating new class of materials with a well-defined periodic arrangement of mesopores.[1] To understand their properties and utilize MCs optimally, it is essential to determine structures of MCs accurately. MCs are formed through co-operative self-assembly of inorganic species with surfactants in water,[2] and thus can be regarded as frozen versions of lyotropic mesophases.[3] Among various techniques for characterizing MC structures, electron tomography and electron crystallography (EC) are the only methods that yield a direct three-dimensional (3D) structural model without geometrical assumptions.[4] When an object is periodic, such as the case of MCs, structural information is localized at reciprocal lattice points, and thus EC is the method of choice. We have developed EC for MCs toward direct 3D reconstruction, which has worked with a resolution of about 1.5 nm.[5–9] All of the silica MCs with cubic symmetry have been solved by EC as 3D electrostatic potential maps (EPMs).[10] Determination of the wall boundary structure from the reconstructed EPM is essential to study the property of the pore structure. To date, the porosity data from gas adsorption analysis and the silica wall density are required for determining the wall structure, which has provoked crucial discussions[11] in terms of limitations of the method.[6,7,12,13]

Herein, we present an approach to obtain a self-consistent structural solution of periodic silica MCs from EC. This is realized by minimizing the Helfrich energy density of the boundary[14] between inorganic and organic mesophase components. The approach relies on an assessment of curvatures along the electrostatic potential surfaces, and adopts the EPM closest to constant mean curvature (CMC) surface as the best determination of mean wall position.[15,16] To interpret and analyze EC data, it is essential to discuss the physical meaning of the reconstructed EPMs. An EPM $\rho(\mathbf{r})$, where $\mathbf{r}$ is a coordinate, is a continuous distribution of electrostatic potential levels. A wall boundary structure is given by a curved surface embedded in the 3D potential map that partitions space into the wall and the mesopore regions; a partition is expressed as an equipotential surface (EPS) defined by a certain potential level c: $\rho(\mathbf{r}) = c$.[5] As MCs are a part of soft matter systems,[17] their mesostructure fluctuates from place to place. Compared to conventional atomistic crystals, the replication of unit cell for MCs is less perfect. This fact causes a rapid decay in amplitudes of the Fourier component with respect to the reciprocal distance. As a consequence, $\rho(\mathbf{r})$ generally shows a broad distribution in 3D space. A schematic explanation is given in Figure S1 in the Supporting Information. This aspect of MCs makes the determination of wall position obscure, and thus the structural solution of MC has to be discussed carefully. We suggest that structural solution of a MC should be described by a representative unit cell reflecting the averaged picture. We rely on an assessment of curvatures (see Computational Methods) to select the EPS characterized by a threshold of c (termed c_T) representing the effective boundary surface as the realistic solution of the underlying MC.

The self-consistency of the present approach allows the evaluation of properties of the mesopore geometry regardless of the presence of remaining surfactants. This is an important advantage for cases that surfactants are designed to remain for stabilizing/protecting molecules, drugs, and peptides. Moreover, the fundamental mesopore information (the mesoscopic surface area and mesoporosity) can be obtained along with the curvature distribution on the determined EPS. Knowledge of local curvatures is also useful information, especially for functional properties of ramified porous structures.[18]

During syntheses of MCs, the polymerization of the silica precursor takes place at the boundary between water and the amphiphile sheet. The amphiphile sheet can be approximated as an elastic continuum, where the Helfrich energy is a good description of the boundary surface energy.[14] The Helfrich energy can be described by the mean curvature H and the Gaussian curvature K.[19] Within the reconstructed EPM, a possible candidate for the boundary surface differentiating the silica wall from the mesopore is expressed by an EPS: $\rho(\mathbf{r}) = c$. The value of c is discussed herein in a rescaled range (0–100%). First, to describe the wall structure, we determine c_T (as the threshold of c for the mean wall structure) by minimizing the Helfrich energy density under the condition of the constant ramification of mesopores; it leads to a CMC scheme (see Computational Methods). The curvature properties are then examined on the determined EPS. Furthermore,

[*] Dr. K. Miyasaka, Prof. O. Terasaki
Graduate School of EEWS (WCU)
Korea Advanced Institute of Science and Technology (KAIST)
Yuseong-gu, Daejeon 305-701 (Republic of Korea)
Fax: (+82) 42-350-1710
E-mail: keii@kaist.ac.kr
Prof. O. Terasaki
Inorganic and Structural Chemistry and EXSELENT
Department of Materials and Environmental Chemistry
Stockholm University, Stockholm 10691 (Sweden)

[**] This work was supported by the Swedish Research Council (VR) and the World Class University (WCU) program (R-31-2008-000-10055-0). We thank S. Hyde, M. Anderson, Y. Sakamoto, N. Fujita, and T. Castle for scientific discussions, and R. Ryoo and S. Che for providing samples.

Supporting information for this article is available on the WWW under http://dx.doi.org/10.1002/anie.201003875.

information about pore fraction and surface complexity as purely mesoscopic measures, denoted f and A, can be obtained (See Computational Methods for a definition of f and A). These properties are fundamental for MCs associated with their applications, such as catalytic properties. In the following, the approach is applied to bicontinuous MCs: MCM-48($Ia\bar{3}d$)[6] and AMS-10($Pn\bar{3}m$).[9]

MCM-48 and AMS-10 consist of bicontinuous interwoven channels. Their silica wall structure follows the periodic minimal G and D surfaces[20,21] (Figure 1). Herein we utilize topology to stand for the mesopore ramification in EPM. The structural topology is related to K integrated over an EPS and characterized by the Euler characteristic χ, which holds constant unless the mesopore ramification changes. For MCM-48, χ in a cubic unit cell changes from -16 to -48 at $c_T = 83.2\,\%$ for the as-synthesized (as-syn) sample, and 92.6 % for calcined (cal) sample, respectively. Such a change in χ of MCM-48 corresponds to the appearance of complementary pores at the flat point (Wyckoff site 16*a*) of the associated G surface penetrating between the distinct subspaces.[8,22] For AMS-10, $\chi = -4$ in a cubic unit cell changes to -8 at $c_T = 95.7\,\%$, generating the connectivity between two distinct channels at Wyckoff site 4*c*. Herein our evaluation is conducted within $\chi = -16$ of MCM-48 and $\chi = -4$ of AMS-10.

As seen in Figure 1 a, the Helfrich energy densities of as-syn-MCM-48 and cal-MCM-48 samples show minima at $c_T = 59.5\,\%$ and 78.3 %, respectively. This value of c_T offers an EPS closest to the CMC surfaces. We simulate the transmission electron micrograph based on the determined wall structure, which agrees well with the experimental observation (Figure 2 a). As summarized in the Supporting Information, Table S1, cal-MCM-48 can accommodate a larger volume of the subspace with lower potential, despite shrinkage of the unit cell. This effect is ascribed to the contraction of the silica wall. On the EPS, the distribution of both ΔH (deviation from the surface-averaged mean curvature, $\Delta H = H - \langle H \rangle$) and of K, are examined as depicted in Figure 3 a,b, where the EPS plots are colored to render the curvature distributions. H of as-syn-MCM-48 surface varies around $\langle H \rangle = 0.20\ \mathrm{nm}^{-1}$ from $0.11\ \mathrm{nm}^{-1}$ to $0.34\ \mathrm{nm}^{-1}$, whilst H of cal-MCM-48 around $\langle H \rangle = 0.13\ \mathrm{nm}^{-1}$ from $0.09\ \mathrm{nm}^{-1}$ to $0.17\ \mathrm{nm}^{-1}$. The wall structure of cal-MCM-48 remains closer to the CMC surface, with a standard deviation of H that is a half of the value of as-syn-MCM-48 (Supporting Information, Table S2). The K distribution displays negative values (up to $-0.50\ \mathrm{nm}^{-2}$) over the entire surface, except in the vicinity of the flat point of as-syn-MCM-48, at which K is positive (maximum $+0.07\ \mathrm{nm}^{-2}$). This result indicates that the shape of the surface around the flat point is concave. The cal-MCM-48 affords a smoother EPS, as supported by the fact that the total area with $K > 0$ of as-syn-MCM-48 exceeds that of the calcined sample (Figure 4 a,b, surface-area-weighted histograms of K). We stress that this is the first structural report that describes EC of MCs whose mesopores are filled by surfactants. Thus we can show the structural change from as-synthesized to calcined silica MC to form the smoother surface.

Figure 1 b shows that AMS-10 has a minimum energy at $c_T = 75.3\,\%$, on the basis of which the wall structure is determined. In Figure 2 b, the simulated transmission electron micrograph is consistent with the observed micrograph. The area around the flat points in AMS-10 also has a slightly concave shape ($0 < K < 0.013\ \mathrm{nm}^{-2}$), similar to MCM-48. In the Supporting Information, Table S1, the smaller A value of AMS-10 compared to MCM-48 indicates lower surface complexity, and thus it can be predicted that AMS-10 may not accord the large surface area property unless the cell size is notably small. This result conforms with the reported BET surface area ($493\ \mathrm{m^2\,g^{-1}}$) of AMS-10.[9] As already implied by the remarkably small Helfrich energy density (Figure 1 b), the local curvature distributions of AMS-10 stay in narrow ranges (Figure 3 c, 4 c). Note that the color-coding for the distribution

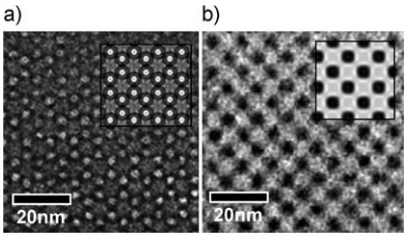

Figure 2. Transmission electron micrographs (adopted from Refs [6] and [9]) are compared with simulated images (inset enclosed by black squares) based on the 3D mesostructure determined by the present approach. a) cal-MCM-48 ($c_T = 78.3\,\%$) along [111], b) AMS-10 ($c_T = 75.3\,\%$) along [100].

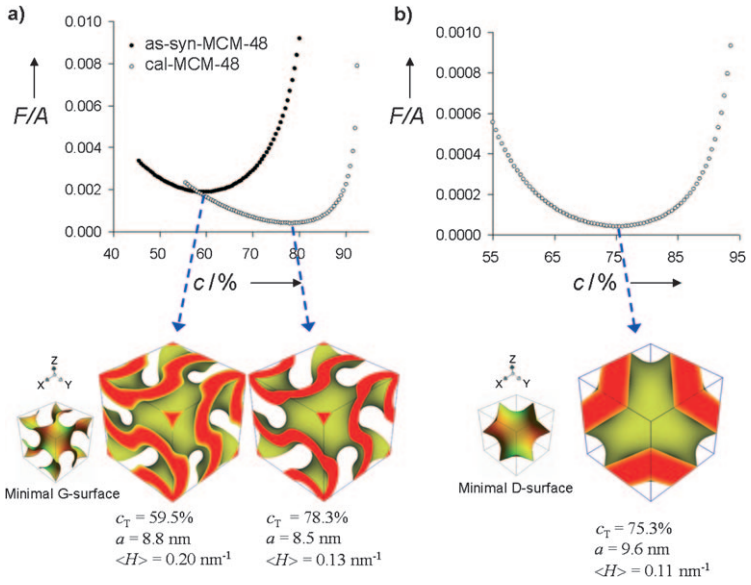

Figure 1. Plot of the Helfrich energy density with respect to *c*, and determined 3D MC solutions. a) MCM-48, and b) AMS-10. The associated periodic minimal surfaces are also shown (to the left of the solutions).

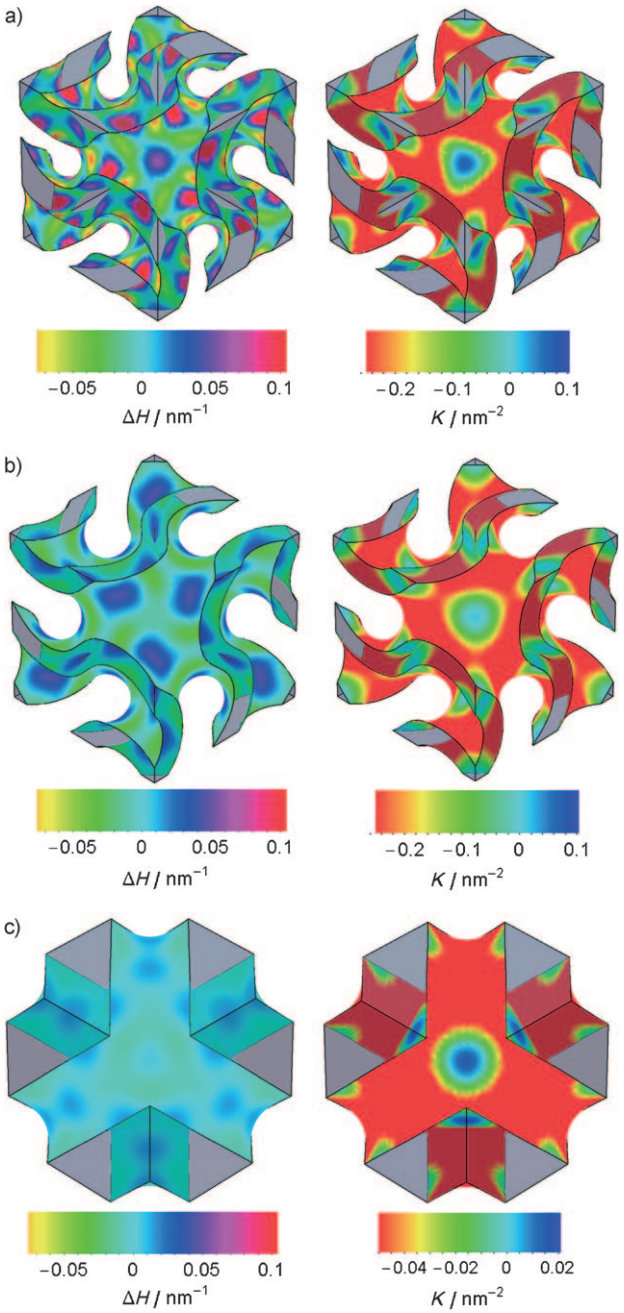

Figure 3. Color-coded distributions of ΔH and K on the obtained EPS viewed along [111]. a) As-syn-MCM-48, b) Cal-MCM-48, and c) AMS-10. The gray color represents the silica wall region.

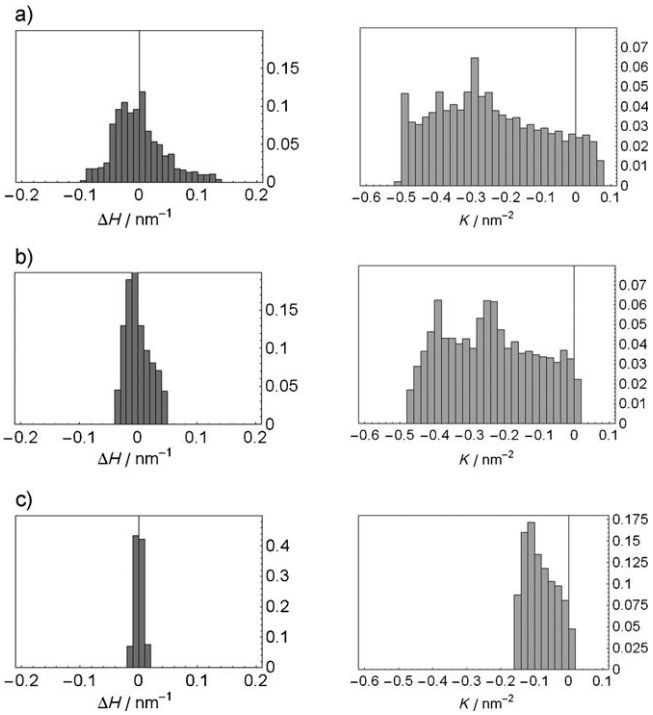

Figure 4. Normalized histograms for the mean curvature deviation (left) and the Gaussian curvature (right) on the EPS. a) As-syn-MCM-48, b) Cal-MCM-48, and c) AMS-10. The frequency of the curvature values is weighted by the area of each surface patch.

of K in AMS-10 is different from the case of MCM-48 to enhance small variances in Figure 3c. H varies from 0.10 nm^{-1} to 0.13 nm^{-1}, and K varies from -0.15 nm^{-2} to $+0.013$ nm^{-2}. These narrow curvature distributions in AMS-10 should be highlighted in comparison with those of MCM-48 structure; AMS-10 has a smoother surface. This comparison does not mean that the AMS-10 mesostructure is energetically favorable than MCM-48 because the elastic moduli [Computational Methods, Eq. (3)] are currently unclear for each material, and thus are not considered in the present study. However, it does mean that the geometry of AMS-10 allows smoother silica wall structure than that of MCM-48. It is worth noting that the G surface shows the greatest global homogeneity among its Bonnet-related cubic minimal surfaces (G, D, and P surfaces), whereas their local homogeneities are nearly identical.[23] This is commensurate, in terms of silica MCs, with the fact that the bicontinuous $Pn\bar{3}m$ is rarely found[9] whereas the bicontinuous $Ia\bar{3}d$ mesostructure is commonly reported. The comparison of the mesostructural stability for MCs is left as a future study.

Finally, we emphasize that a physical meaning of an EPS for silica MCs is "an effective partitioning surface between silica wall and void space upon the averaged distribution of 3D EPM". We have demonstrated the determination of appropriate EPSs representing MC structures based on the CMC scheme, which was conducted without any other porosity experiments. This approach is amenable to a self-consistent structural solution within the EPM data of an underlying MC reconstructed by EC, and applicable to any mesoporous including cage-type, or indeed macroporous, crystals where surface boundary energy drives self-organization. The curvature assessment for H and K illuminates the detailed geometry of the silica wall structure. Direct nanoscopic information of the mesopore volume and surface area from EC can consequently suggest the representative pore properties for what may be a heterogeneous sample. It gives a new insight in understanding structural properties of periodic but somewhat deviating mesostructures.

Computational Methods

Calculating curvature, surface area, and pore volume: A surface normal to an EPS $\rho(\mathbf{r})=c$ at any point is defined by $\mathbf{n}=\nabla\rho/|\nabla\rho|$, and from this the mean curvature $H(\mathbf{r})$ and the Gaussian curvature $K(\mathbf{r})$ are given by Equations (1,2):

$$H(\mathbf{r})=\frac{\mathrm{div}\,\mathbf{n}}{2} \tag{1}$$

$$K(\mathbf{r})=\frac{1}{2}\left\{(\mathrm{div}\,\mathbf{n})^2+(\mathrm{rot}\,\mathbf{n})^2-\sum_{i,j}(\partial_i n_j)^2\right\} \tag{2}$$

The Helfrich energy per unit area is formulated in terms of $H(\mathbf{r})$ and $K(\mathbf{r})$ [Eq. (3)]:

$$2\kappa_1(H(\mathbf{r})-H_0)^2+\kappa_2 K(\mathbf{r}) \tag{3}$$

where H_0 represents the spontaneous curvature, κ_1 and κ_2 are the bending and the saddle-splay elastic moduli, respectively. The Gauss–Bonnet theorem claims that the integral of $K(\mathbf{r})$ over the surface remains constant [Eq. (4)]:

$$\frac{1}{2\pi}\int\int K(\mathbf{r})\mathrm{d}A=\chi \tag{4}$$

where χ is the Euler characteristic and related merely to the topology of the structure. Thus when the topology does not change, a term of the Gaussian curvature is dropped in Equation (3). The dimensionless Helfrich energy is then given by Equation (5):

$$F=\int\int (H(\mathbf{r})-H_0)^2\mathrm{d}A \tag{5}$$

Note that we do not take the bending elastic moduli in Equation (5) as its dependence on a material is unknown, which restricts the evaluation to become valid within respective data of EPM. The weighted average of $(H(\mathbf{r})-H_0)^2$ is given by F/A, where A denotes the area over the surface [Eq. (6)]:

$$A=\int\int \mathrm{d}A \tag{6}$$

The formulation of F/A is equivalent to the variance of the mean curvature distribution from H_0, which gives rise to the dependence on the frequency distribution of $H(\mathbf{r})$ over the surface. To determine H_0, we adopt the weighted average of $H(\mathbf{r})$ over the surface so that the most probable value is obtained. Thereby, H_0 in Equation (5) is expressed as in Equation (7):

$$H_0=\langle H\rangle=\frac{1}{A}\int\int H(\mathbf{r})\mathrm{d}A \tag{7}$$

which will give a scheme of constant mean curvature surface. It should be noted that H_0 is generally non-uniform and a function of position and curvature. We however handle H_0 as a constant for simplicity.

The pore (or surfactant) subspace volume relative to a^3, f, and the surface area relative to a^2, A, are fundamental quantities for porous media. They are estimated from the 3D model of the EPS as Equation (8):

$$f=\frac{1}{3}\int\int \mathbf{r}\cdot\mathbf{n}\mathrm{d}A \tag{8}$$

and Equation (6), respectively. Those values for the present mesostructures are tabulated in the Supporting Information, Table S2.

Code for the above calculations was implemented by KM using Mathematica version 6 (Wolfram Research, Inc.) It is presumed that the assessment is based on a mesoscopic measure, in which the structure is handled as a continuum body, and its boundary surface is atomistically smooth.

Image simulation: Transmission electron micrographs of MCM-48 and AMS-10 were simulated using MacTempasX software program (Total Resolution LLC) based on the multislice method. MacTempasX requires the input file based on the atomistic structural model. We prepared the input file by placing a silicon atom randomly within the wall space of the mesostructures determined by the present approach (Figure 1) on condition that the average density remains 2.2 $\mathrm{g\,cm^{-3}}$.[24] The specimen thickness of 40 nm and the defocus values of −320 nm for MCM-48 and that of −640 nm for AMS-10 were assumed as those values mimic the experimental transmission electron microscopy observations. The scattering vectors whose norm was less than 5 $\mathrm{nm^{-1}}$ were included during the multislice diffraction calculation, and those less than 1 $\mathrm{nm^{-1}}$ were used to form the resultant images. The accelerating voltage and spherical aberration were set to be 300 kV and 0.6 mm, respectively, as employed during observations made in the literature.[6,9]

Received: June 25, 2010
Published online: October 12, 2010

Keywords: electron crystallography · Gaussian curvature · Helfrich energy · mean curvature · mesoporous crystals

[1] C. T. Kresge, M. E. Leonowicz, W. J. Roth, J. C. Vartuli, J. S. Beck, *Nature* **1992**, *359*, 710.
[2] K. J. Edler, *Aust. J. Chem.* **2005**, *58*, 627.
[3] K. Larsson, F. Tiberg, *Curr. Opin. Colloid Interface Sci.* **2005**, *9*, 365.
[4] M. W. Anderson, T. Ohsuna, Y. Sakamoto, Z. Liu, A. Carlsson, O. Terasaki, *Chem. Commun.* **2004**, 907.
[5] Y. Sakamoto, M. Kaneda, O. Terasaki, D. Y. Zhao, J. M. Kim, G. Stucky, H. J. Shim, R. Ryoo, *Nature* **2000**, *408*, 449.
[6] M. Kaneda, T. Tsubakiyama, A. Carlsson, Y. Sakamoto, T. Ohsuna, O. Terasaki, S. H. Joo, R. Ryoo, *J. Phys. Chem. B* **2002**, *106*, 1256.
[7] A. E. Garcia-Bennett, K. Miyasaka, O. Terasaki, S. N. Che, *Chem. Mater.* **2004**, *16*, 3597.
[8] Y. Sakamoto, T. W. Kim, R. Ryoo, O. Terasaki, *Angew. Chem.* **2004**, *116*, 5343; *Angew. Chem. Int. Ed.* **2004**, *43*, 5231.
[9] C. B. Gao, Y. Sakamoto, K. Sakamoto, O. Terasaki, S. N. Che, *Angew. Chem.* **2006**, *118*, 4401; *Angew. Chem. Int. Ed.* **2006**, *45*, 4295.
[10] O. Terasaki, T. Ohsuna, Z. Liu, Y. Sakamoto, A. E. Garcia-Bennett, *Stud. Surf. Sci. Catal.* **2004**, *148*, 261.
[11] The wall structure may not be determined when the pore is not accessible by gas molecules, such as as-synthesized materials or pore-blocked materials.
[12] Y. Sakamoto, I. Diaz, O. Terasaki, D. Y. Zhao, J. Perez-Pariente, J. M. Kim, G. D. Stucky, *J. Phys. Chem. B* **2002**, *106*, 3118.
[13] P. I. Ravikovitch, A. V. Neimark, *Langmuir* **2002**, *18*, 1550.
[14] W. Helfrich, *Z. Naturforsch.* **1973**, *28c*, 693.
[15] E. J. Siem, W. C. Carter, *Interface Sci.* **2002**, *10*, 287.
[16] M. W. Anderson, P. J. Hughes, O. Terasaki, Y. Sakamoto, K. Brakke, *Stud. Surf. Sci. Catal.* **2007**, *165*, 13.
[17] R. Holyst, *Soft Matter* **2005**, *1*, 329.
[18] Z. Blum, S. T. Hyde, B. W. Ninham, *J. Phys. Chem.* **1993**, *97*, 661.
[19] S. T. Hyde, S. Andersson, K. Larsson, Z. Blum, T. Landh, S. Lidin, B. W. Ninham, *The Language of Shape*, Elsevier Science B.V., Amsterdam, **1997**.
[20] A. H. Schoen, NASA Technical Note D-5541, **1970**.
[21] E. A. Lord, A. L. Mackay, *Curr. Sci.* **2003**, *85*, 346.
[22] T. W. Kim, F. Kleitz, B. Paul, R. Ryoo, *J. Am. Chem. Soc.* **2005**, *127*, 7601.

[23] G. E. Schröder-Turk, A. Fogden, S. T. Hyde, *Eur. Phys. J. B* **2006**, *54*, 509.
[24] This value of silica wall density is widely accepted for calcined MCs. The wall density of as-synthesized MCs should be lower because the presence of Si–OH termination makes the silica wall less condensed. For this image simulation, however, we assumed the same density for both as-synthesized and calcined MCs, as the precise value is unclear as yet, and a decrement of the average wall density of MCs only changes the contrast range that is adjustable for the sake of comparison with the observed images.

